Demonstration of high Raman gain in a submicrometer-size silicon-on-insulator waveguide

Qianfan Xu, Vilson R. Almeida, and Michal Lipson

School of Electrical and Computer Engineering, Cornell University, 411 Phillips Hall, Ithaca, New York 14853

Received June 22, 2004

We show high Raman gain in a silicon submicrometer-size planar waveguide. Using high-confinement structures and picosecond pump pulses, we show 3.1-dB net internal gain with 2.8-W peak pump power in a 7-mm-long waveguide. We also analyze experimentally and theoretically the effect of free-carrier absorption on the Raman gain. © 2005 Optical Society of America

OCIS codes: 230.7370, 250.4480, 190.4390.

Silicon-on-insulator (SOI) waveguides are a promising platform for monolithically integrating various optical devices with electronics. However, light emission and amplification are difficult to achieve on silicon owing to its indirect bandgap. Stimulated Raman scattering could be used for overcoming this limitation of silicon as an active device, taking advantage of the high Raman-scattering efficiency[1] in crystalline silicon.[1] Raman gain in silicon was shown to be limited by absorption from free carriers generated by two-photon absorption (TPA) at a high pump power.[2,3] In this Letter we demonstrate a Raman gain of 5.6 dB with a 3.1-dB net internal gain in silicon in a 7-mm-long submicrometer strip waveguide with 2.8-W pump power. The high confinement strongly increases the intensity of the pump light and therefore increases the Raman gain. To isolate the Raman effect from the free-carrier absorption (FCA) effect, we use a pulsed pumping scheme that prevents free carriers from building up over time and masking the Raman gain.

The structure used here for measuring gain in silicon is a 7-mm-long strip SOI waveguide. The core of the waveguide has a height of 230 nm and a width of 440 nm. The structure was fabricated with a process similar to that described in Ref. 4. The modal area of the quasi-TM mode is 0.18 μm^2 at the wavelength of 1480 nm calculated by simulation of the mode profile of the waveguide with a full-vectorial finite-difference mode solver.[5] The propagation loss of the waveguide is estimated by the paper-clip method[6] to be 2.5 dB/cm for the quasi-TM mode and 5.2 dB/cm for the quasi-TE mode.

In our experiments the pump and probe beams are coupled to the waveguide by nanotapers.[4] The coupling loss is approximately 2 dB. The pump light is generated by an optical parametric oscillator and is then filtered by a Fabry–Perot filter to extend the pulse width. The resulting pump pulse has a repetition rate of 76.8 MHz and a FWHM of 3.6 ps with a single-sided exponential shape, measured with the autocorrelator. The pump pulse is transform limited with a 0.45-nm-FWHM Lorentzian spectrum. In the experiment the pump wavelength is fixed at $\lambda_{pump} = 1480.0$ nm. A cw tunable laser with less than 1-MHz linewidth is used as the probe. Since the optical phonon in silicon has a frequency of 15.6 THz and a bandwidth of 105 GHz,[1] the central wavelength and bandwidth of the Raman gain in the waveguide are expected to be $\lambda_0 = 1603.5$ nm and $\Delta\lambda = 0.9$ nm, respectively.

Figure 1(a) shows the transmission of the probe in quasi-TE mode measured with a pump pulse in quasi-TM mode. The cw probe wavelength is $\lambda_{probe} = 1603.4$ nm. The pump light has an average power of 1.3 mW at the input of the waveguide, corresponding to a peak power of 2.8 W. On the transmission waveform we see an increase in probe transmission corresponding to net internal gain when the pump pulse passes through the waveguide. The

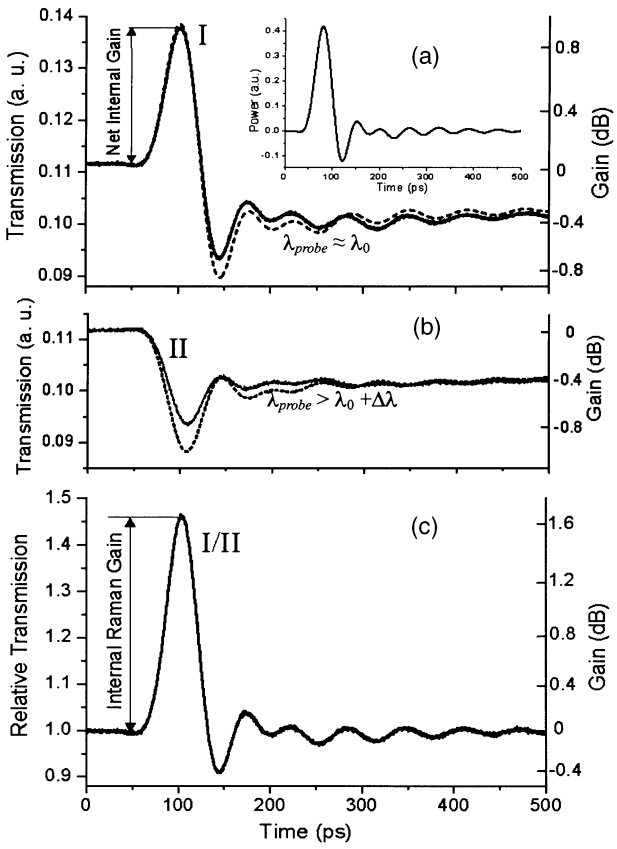

Fig. 1. Measurement-limited probe transmission waveform for the wavelengths of 1603.5 nm [solid curve in (a)] and 1605.4 nm [solid curve in (b)]. The dashed curves in (a) and (b) are the results of simulations. The inset in (a) shows the response of the detector to the pump pulse. (c) Relative transmission obtained by dividing curve I in (a) by curve II in (b).

0146-9592/05/010035-03$15.00/0

waveform is limited by the slow (~30-ps) response time of the 12-GHz detector. The peak value of the measurement-limited net internal gain is 0.9 dB. The ripples in the waveform are also due to the response of the detector. In the inset of Fig. 1(a) we show the response of the detector to a single pump pulse, where one can see the same pattern of ripples.

The net internal gain is a combined effect of the gain that is due to the Raman effect and the loss caused by TPA and FCA effects in the waveguide. To isolate the Raman effect from the TPA and FCA effects, we measure the probe transmission when $\lambda_{\text{probe}} = 1605.4\ \text{nm} > \lambda_0 + \Delta\lambda$, where the Raman gain is expected to be minimum [Fig. 1(b)], whereas the nonlinear absorptions are expected to be almost identical. The magnitude of the FCA and the free-carrier lifetime can be obtained from the exponential fitting of the decay of the nonlinear absorption after the pump pulse has passed. Using this method, we find the free-carrier lifetime in the waveguide to be 1.37 ns, which is much smaller than that in bulk silicon because of the carrier recombination at the $Si-SiO_2$ interfaces. The measurement-limited internal Raman gain on the probe beam is shown in Fig. 1(c), corresponding to the difference between the waveforms shown in Figs. 1(a) and 1(b).

The net internal gain is limited by the FCA at high pump powers, since the free carriers are generated by TPA,[7] and the carrier density is proportional to the square of the pump intensity. We show in Fig. 2 the measurement-limited internal Raman gain [see Fig. 1(c)], the free-carrier absorption, and the net measurement-limited internal gain [see Fig. 1(a)] versus the peak power of the pump pulse. The error bars originate from the error in the estimation of the peak power and in the alignment of Figs. 1(a) and 1(b) for obtaining the internal Raman gain. One can see from the figure that, when the pump power is low, the internal Raman gain increases linearly with the pump power, whereas the FCA increases superlinearly. When the pump power is high (>~1.3 W), because the pump pulses experience extra loss from TPA and FCA,[5] the increase in both the internal Raman gain and the FCA is slower. One can see that the net internal gain saturates at a high pump power (~2.3 W).

To measure the bandwidth of the Raman gain, we extract the Raman gain from the transmission waveform at each probe wavelength. In Fig. 3 we show the measurement-limited internal Raman gain versus the probe wavelength when the peak power of the input pump pulse is 1.2 W. The gain spectrum is fitted with a Lorentzian spectrum shape, which is shown as the solid curve in Fig. 3. The central wavelength of the gain spectrum is $\lambda_0 = 1603.6$ nm and the FWHM linewidth is $\Delta\lambda = 0.91 \pm 0.07$ nm. These values agree well with previously published values measured for rib waveguides.[1]

From the FWHM of gain spectrum $\Delta\lambda$ and its Lorentzian shape we extract the phonon lifetime in silicon of $\tau_R = 3$ ps from[8]

$$\tau_R = \frac{{\lambda_0}^2}{\pi c \Delta\lambda}. \tag{1}$$

From this value and the 3.6-ps pump pulse duration we estimate the actual duration of Raman gain to be much shorter than the 37.5-ps Raman gain FWHM measured from the waveform in Fig. 1(c), which is limited by the slow response of the detector. The shorter Raman gain duration implies a higher peak value of Raman gain than that extracted in Fig. 1(c).

To obtain the actual (i.e., non-measurement-limited) value of peak Raman gain and net internal gain, we simulate the Raman gain dynamics in the waveguide with the following rate equations:

$$\frac{\partial I_P(\mathbf{r},t)}{\partial z} + \frac{c}{n_{gP}}\frac{\partial I_P(\mathbf{r},t)}{\partial z} = -\gamma_P I_P(\mathbf{r},t) - \alpha_P n(\mathbf{r},t) I_P(\mathbf{r},t) - \beta I_P(\mathbf{r},t)^2 - g_R I_P'(\mathbf{r},t) I_S(\mathbf{r},t)\frac{\omega_P}{\omega_S}, \tag{2}$$

$$\frac{\partial I_S(\mathbf{r},t)}{\partial z} + \frac{c}{n_{gS}}\frac{\partial I_S(\mathbf{r},t)}{\partial z} = -\gamma_S I_S(\mathbf{r},t) - \alpha_S n(\mathbf{r},t) I_S(\mathbf{r},t) - 2\beta I_P(\mathbf{r},t) I_S(\mathbf{r},t) + g_R I_P'(\mathbf{r},t) I_S(\mathbf{r},t), \tag{3}$$

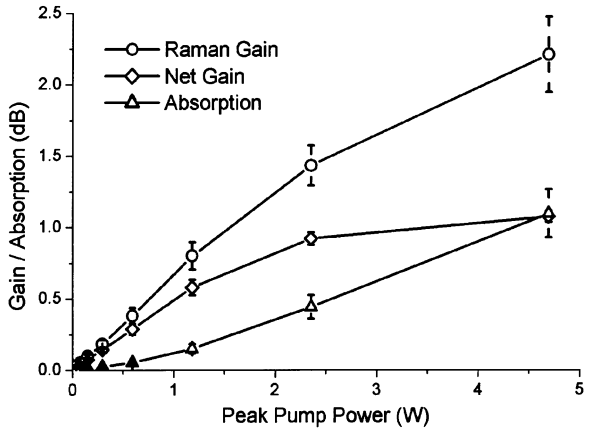

Fig. 2. Measurement-limited internal Raman gain (curve with circles), net internal gain (curve with diamonds), and FCA (curve with triangles) versus pump peak power.

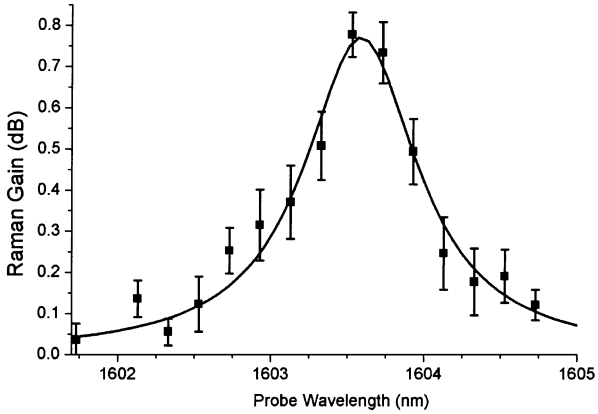

Fig. 3. Measurement-limited Raman gain spectrum. Squares correspond to the peak value of Raman gain extracted from the probe transmission. The solid curve corresponds to the fitted Lorentzian spectrum.

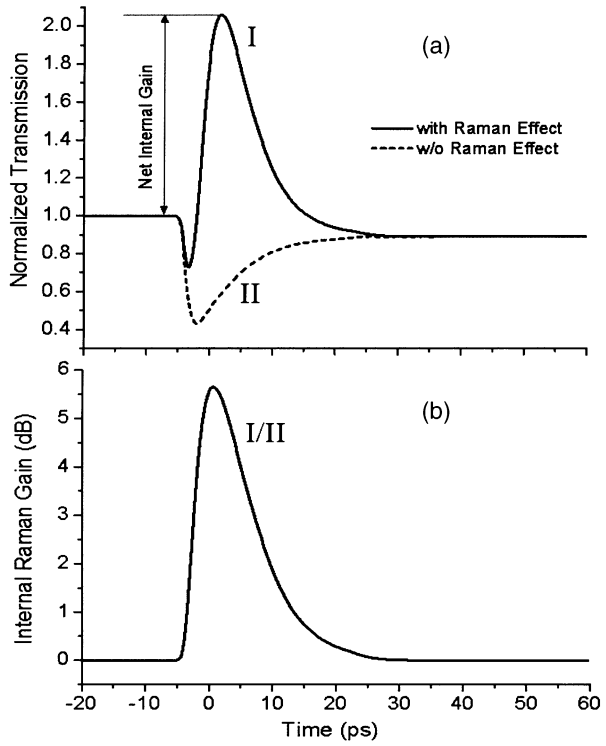

Fig. 4. Gain dynamics obtained from simulation. (a) Normalized probe transmission when the Raman effect is present and when it is not present. (b) Raman gain obtained by dividing the solid curve in (a) by the dashed curve in (b).

where I_P and I_S are the local pump and probe intensities, respectively; z is the transmission direction of the waveguide; n_{gP} and n_{gS} are the group indices of pump and probe, respectively, obtained from the finite-difference mode solver[5]; γ_P and γ_S are the linear transmission losses of the waveguide for pump and probe, respectively; $\alpha_P = 1.32 \times 10^{-17}$ cm^2 and $\alpha_S = 1.55 \times 10^{-17}$ cm^2 are the FCA coefficients of pump and probe, respectively[3]; n is the local free-carrier density; $\beta = 0.79$ cm/GW is the TPA coefficient[9]; $g_R = 4.2$ cm/GW is the Raman gain coefficient; and I_P' is the effective pump power that contributes to the phonon density at time t:

$$I_P'(\mathbf{r},t) = \int_{-\infty}^{t} I_P(\mathbf{r},t)\,\frac{1}{\tau_R}\exp\!\left(-\frac{t-\tau}{\tau_R}\right)\mathrm{d}\tau\,. \qquad (4)$$

In the simulation the transverse mode profiles of both the pump and the probe are obtained from the finite-difference mode solver and are assumed to be unchanged over z.

To compare the simulation results with the experimental results, we calculate the detector response by convoluting the gain dynamics found from the simulation with the impulse response of the detector. The results are shown as dashed curves in Figs. 1(a) and 1(b) for the Raman effect included and not included in the simulation, respectively. One can see that the simulation agrees well with the experimental result. The value of g_R used in the simulation is lower than the previously reported value of 20 cm/GW.[1] The lower gain coefficient may be due to the different type of waveguide used, with different strain levels and surface effects.

The gain dynamics obtained from the simulations are shown in Fig. 4. The solid curve in Fig. 4(a) shows the relative transmission of the probe when the Raman effect is present. One can see a 3.1-dB net internal gain on the waveform. The dashed curve in Fig. 4(a) shows the transmission when there is no Raman effect, corresponding to the situation when the probe is out of the Raman bandwidth. A comparison of the two waveforms in Fig. 4(a) allows the internal Raman gain to be obtained, and it is shown in Fig. 4(b). We find the peak internal Raman gain to be 5.6 dB.

In conclusion, we have observed high net gain from the Raman effect with a highly confined strip SOI waveguide and short-pulse pumping. The gain can be used to amplify the return-to-zero signal in a telecommunication system, compensate for nonlinear losses in an all-optical switch based on silicon, and pump as well as actively mode lock a silicon-based laser.

This work was supported by the U.S. Air Force Office of Scientific Research under grant AFOSR F49620-03-1-0424. The experiments were performed at the Cornell Center for Nanoscale Systems, supported by the Nanoscale Science and Engineering Initiative of the National Science Foundation under award EEC-0117770 and the New York State Office of Science, Technology, and Academic Research under contract C020071. M. Lipson's e-mail address is lipson@ece.cornell.edu.

References

1. R. Clap, D. Dimitropoulos, V. Raghunathan, Y. Han, and B. Jalali, Opt. Express **11,** 1731 (2003), http://www.opticsexpress.org.
2. T. K. Liang and H. K. Tsang, in *Conference on Lasers and Electro-Optics, International Quantum Electronics Conference, and Photonic Applications Systems Technologies Technical Digest on CD-ROM* (Optical Society of America, Washington, D.C., 2004), paper CThT48.
3. R. Claps, V. Raghunathan, D. Dimitropoulos, and B. Jalali, Opt. Express **12,** 2774 (2004), http://www.opticsexpress.org.
4. V. R. Almeida, R. R. Panepucci, and M. Lipson, Opt. Lett. **28,** 1302 (2003).
5. C. L. Xu, W. P. Huang, M. S. Stern, and S. K. Chaudhuri, IEE Proc. Optoelectron. **141,** 281 (1994).
6. S. J. Spector, M. W. Geis, D. M. Lennon, R. C. Williamson, and T. M. Lyszczarz, in *Integrated Photonics Research Topical Meetings on CD-ROM* (Optical Society of America, Washington, D.C., 2004), paper ITHE5.
7. T. K. Liang and H. K. Tsang, Appl. Phys. Lett. **84,** 2745 (2004).
8. P. J. Delfyett, R. Dorsinville, and R. R. Alfana, Opt. Lett. **12,** 1002 (1987).
9. M. Dinu, F. Quochi, and H. Garcia, Appl. Phys. Lett. **82,** 2954 (2003).